

# Linköping University Post Print

## Effective Suppression of Surface Recombination in ZnO Nanorods Arrays during the Growth Process

Li-Li Yang, Qingxiang Zhao, Magnus Willander, Xianjie Liu, Mats Fahlman and J H Yang

N.B.: When citing this work, cite the original article.

This document is the Accepted Manuscript version of a Published Work that appeared in final form in *CRYSTAL GROWTH and DESIGN*, copyright © American Chemical Society after peer review and technical editing by the publisher.

To access the final edited and published work see:

Li-Li Yang, Qingxiang Zhao, Magnus Willander, Xianjie Liu, Mats Fahlman and J H Yang, Effective Suppression of Surface Recombination in ZnO Nanorods Arrays during the Growth Process, 2010, *CRYSTAL GROWTH and DESIGN*, (10), 4, 1904-1910.

<http://dx.doi.org/10.1021/cg100017b>

Copyright: The American Chemical Society

<http://pubs.acs.org/>

Postprint available at: Linköping University Electronic Press

<http://urn.kb.se/resolve?urn=urn:nbn:se:liu:diva-54866>

# Effective suppression of surface recombination in ZnO nanorods arrays during the growth process

*L.L. Yang*<sup>\*,†,‡</sup>, *Q.X. Zhao*<sup>†</sup>, *M. Willander*<sup>†</sup>, *X.J. Liu*<sup>§</sup>, *M. Fahlman*<sup>§</sup>, *J.H. Yang*<sup>‡</sup>

<sup>†</sup> Department of Science and Technology (ITN), Linköping University, SE-60174  
Norrköping, Sweden

<sup>‡</sup> Institute of Condensed State Physics, Jilin Normal University, Siping, 136000,  
People's Republic of China

<sup>§</sup> Department of Physics, Chemistry and Biology (IFM), Linköping University, SE-  
581 83 Linköping, Sweden

\*E-mail address: [Lili.Yang@itn.liu.se](mailto:Lili.Yang@itn.liu.se)

## RECEIVED DATE

## CORRESPONDING AUTHOR FOOTNOTE

\* Corresponding author: E-mail: [Lili.Yang@itn.liu.se](mailto:Lili.Yang@itn.liu.se), Tel: +46 11 363441.

<sup>†</sup> ITN, Linköping University

<sup>‡</sup> Jilin Normal University

<sup>§</sup> IFM, Linköping University

**Abstracts:**

ZnO nanorods arrays are respectively prepared under different vapor pressure with opening (OZN) or sealing the beaker (SZN). The results from time-resolved photoluminescence measurements indicate that sealing the beaker during the growth process can effectively suppress the surface recombination of ZnO nanorods and the suppression effect is even better than a 500°C post-thermal treatment to OZN. The results from X-ray photoelectron spectroscopy measurement reveal that the main reason for this phenomenon is that the surfaces of SZN are attached by groups related to NH<sub>3</sub> instead of the main surface recombination centers such as OH and H groups in OZN. The ammonia surface treatment on both OZN and SZN samples further testifies that the absorption of the groups related to NH<sub>3</sub> has no contribution to the surface recombination on the ZnO nanorods.

## Introduction

It is well known that surface recombination through surface/interface states is a major loss mechanism for photo-generated carriers, and its negative influence on the photonic devices will become stronger as the geometrical dimension of materials is reduced. In recent decade years, quasi-one-dimensional ZnO nanostructures (e.g. nanorods, nanotubes and nanobelts) have been widely investigated due to their promising applications for nanophotonic applications such as nanolasers [1–3], optical waveguides [4–6], and light emitting diodes [7]. To optimize devices based on ZnO nanostructures, it is necessary to understand the surface recombination mechanisms and explore effective way to control it. But the corresponding investigations about ZnO surface recombination in the emission process and related surface defects are very limited [8-9].

As our previously report about ZnO nanorods grown by two-step chemical bath deposition method, post annealing is an efficient way to suppress the surface recombination process [10-11]. However, this requires high temperature (500°C), which undoubtedly increases the cost of the practical application. In addition, it is not possible to apply such post-grown thermal treatment for some applications which require flexible polymer substrates. From this point of view, if one can explore a way during the low-temperature growth process which can realize the suppression of the surface recombination without changing the properties of the ZnO nanorods, it will not only simplify the preparation procedure of the samples with high crystal quality, but also save the cost for large-scale fabrication.

Therefore, in this paper, we present an easier way to improve the surface quality during the growth process of ZnO nanorods. ZnO nanorods arrays are respectively prepared under different vapor pressure with opening or sealing the beaker. The

results show that the surface quality can strongly be improved through sealing the beaker during the growth, which realizes even better suppression effect on the surface recombination than a 500°C post-thermal treatment to the sample grown in an open beaker. The improvement mechanism of surface quality is also discussed in detail.

## **Experimental section**

The ZnO nanorods arrays used in this investigation were grown on Si substrates by the CBD method, which includes a two-steps process, i.e. a substrate treatment prior to the CBD growth. The substrates were pre-treated by coating the substrate for different times with a 5 mM solution of zinc acetate dihydrate ( $\text{Zn}(\text{OOCCH}_3)_2 \cdot 2\text{H}_2\text{O}$ ) dissolved in pure ethanol. In the CBD growth, 0.1M aqueous solutions of zinc nitrate hexahydrate [ $\text{Zn}(\text{NO}_3)_2 \cdot 6\text{H}_2\text{O}$ , 99.9% purity] and 0.1M aqueous solutions of methenamine ( $\text{C}_6\text{H}_{12}\text{N}_4$ , 99.9% purity) were first prepared and mixed together. The pre-treated Si substrates were immersed in the aqueous solution and kept at 93°C for 2h. During the process of two-steps CBD, many parameters can influence the structure, morphology and properties of the samples, such as seed layer and pH value of chemical solution [12-13]. But in our case, the only difference between two as-grown ZnO nanorods arrays during the growth processes is that the beaker is sealed or not. The sample grown in the open beaker is named OZN; the other grown in the sealed beaker is named SZN. After growth, a part of the OZN was annealed at 500°C for 1h in air atmosphere (named as OZN-A). Furthermore, SZN and OZN are both surface modified in 0.1 M (10ml) ammonia solution at 93°C for 15min (named as OZN-N and SZN-N respectively).

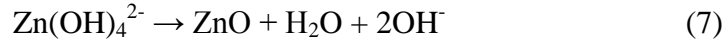
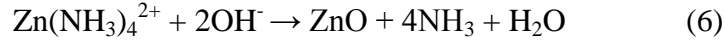
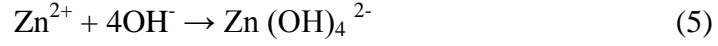
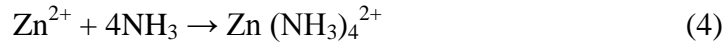
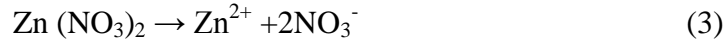
Scanning electron microscopy (SEM) pictures were recorded by using a JEOL JSM-6301F. Photoluminescence (PL) measurements were carried out at room

temperature. A CCD detector (Spectrum One) and a monochromator HR460 from Jobin Yvon-Spex were used to disperse and detect the ZnO emission. Laser line with a wavelength of 266 nm from a diode laser (Coherent Verdi) pumped resonant frequency doubling unit (MBD 266) is used as excitation source. Time resolved PL (TRPL) was performed by using an excitation laser line from a frequency tripled sapphire:Ti laser emitting at 266 nm, a 0.3 m monochromator and a streak camera at 1.8 K. X-ray photoelectron spectroscopy (XPS) measurements were performed using a Scienta® ESCA200 spectrometer in ultra-high vacuum (UHV) with a base pressure of  $10^{-10}$  mbar. The measurement chamber is equipped with a monochromatic Al ( $K\alpha$ ) X-ray source providing photon with  $h\nu=1486.6$  eV. The XPS experimental condition was set so that the full width at half maximum (FWHM) of the clean Au  $4f_{7/2}$  line was 0.65 eV. All spectra were measured at a photoelectron take-off angle of  $0^\circ$  (normal emission) and room temperature. The binding energies were obtained referenced to the Fermi level with an error of  $\pm 0.1$  eV.

## Results and discussion

The SEM images of the as-grown OZN and SZN are shown in Fig.1. The ZNAs were vertically aligned on the Si (001) substrates. The length of SZN (730 nm) is almost twice of OZN (420 nm), which indicates that their growth speeds are different since the two samples are grown for the same time of 2h. In order to see it clearly, two sets of OZN and SZN samples grown for different time are prepared. The length dependence on the growth time is illustrated in Fig. 2, which clearly shows that the growth speed of SZN is almost twice as fast as that of OZN. According to OZN, the reactions in solution can be described by the following formulae [14-16] :





$\text{C}_6\text{H}_{12}\text{N}_4$ , which is extensively used in the fabrication of ZnO nanostructures, provides the hydroxide ions ( $\text{OH}^-$ ) and the ammonia molecules ( $\text{NH}_3$ ) to the solution. Under the open environment, the  $\text{NH}_3$  and  $\text{H}_2\text{O}$  will constantly evaporate from the solution during the whole growth process. On the contrary, when the beaker is sealed, all the  $\text{NH}_3$  and  $\text{H}_2\text{O}$  vapor can not evaporate outside so that the pressure in the beaker increases. Besides, more  $\text{NH}_3$  will participate in the growth of the ZnO nanorods. These two factors finally result in that growth speed of SZN is faster than that of OZN.

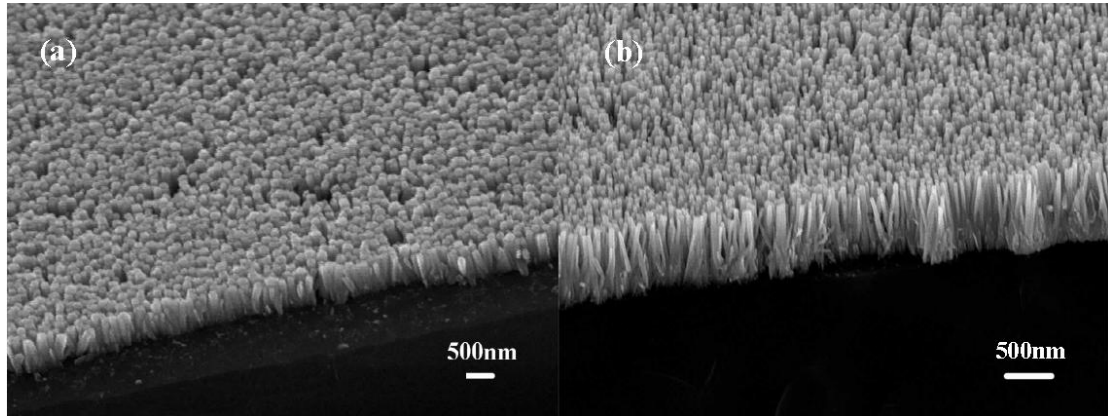


Fig.1 SEM images of OZN (a) and SZN (b) at a 45°C tilted stage.

Fig.3 shows the room temperature PL spectra of OZN, OZN-A and SZN, which consists of a dominant UV peak at 385 nm in wavelength and a very weak and broad deep level emission (DLE) band in the range of 500-600 nm. The UV emission band

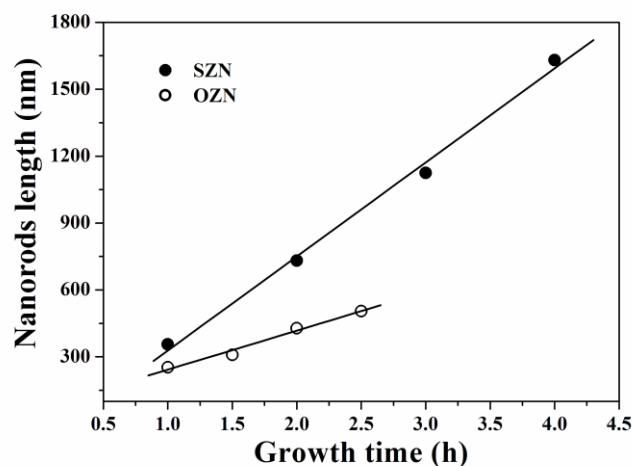


Fig.2 Length dependence of ZnO nanorods as a function of growth time

is related to a near band-edge transition of ZnO, namely, a combination of free exciton and free exciton LO phonon replica emissions. The DLE band has previously been attributed to intrinsic defects in the crystal structure such as O-vacancy ( $V_O$ ) [17-19], Zn-vacancy ( $V_{Zn}$ ) [20-22], O-interstitial ( $O_i$ ) [23] or Zn-interstitial ( $Zn_i$ ) [24]. Recently, this deep level emission band had been identified and at least two different defect origins ( $V_O$  and  $V_{Zn}$ ) with different optical characteristics were claimed to contribute to this DLE band [25-27]. As shown in Fig.3, a remarkable strong enhancement of UV emission intensity appeared in OZN-A and SZN by almost a factor of 4~5 compared to the OZN, and on the contrary the deep level emission band had no big change. We would like to point out that the PL measurements were done in back-scattering geometry, i.e. all the samples are excited from the front top by a laser line with a wavelength of 266nm. The measurements from one sample to another sample were achieved by moving the sample holder and the laser focus and emission collection were optimized every time in order to avoid any intensity variation due to the measurement alignment. In addition, in order to check the consistency of the spectra across the samples, we also have measured different positions across the

samples to do the spatial analysis. The results from different positions are similar. This is consistent with the homogeneity of the samples as shown in the SEM image (see Fig.1). Furthermore, according to the absorption coefficient of ZnO, the penetration depth of the laser is about 300nm, which is shorter than the length of ZnO nanorods in all the samples. Therefore, the emission intensity in PL spectra is only related to the crystal quality of the samples.

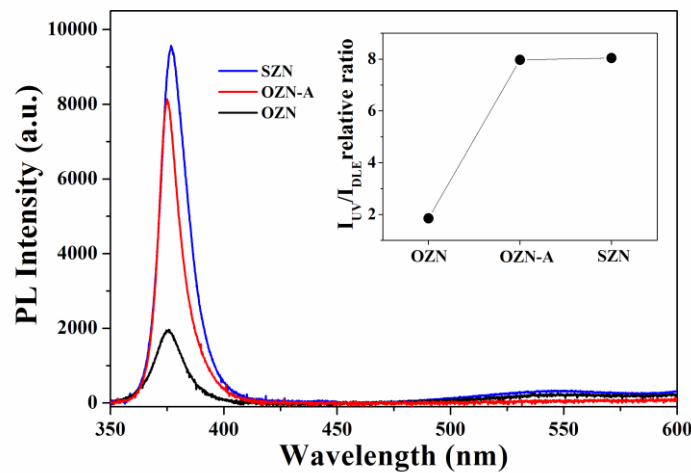


Fig.3 Room temperature PL spectra of OZN, OZN-A and SZN. Insert is the corresponding  $I_{UV}/I_{DLE}$  value.

The relative integrated PL intensity ratio between the UV ( $I_{UV}$ ) and DLE ( $I_{DLE}$ ) can be used to characterize the qualitative deep level defect concentration of ZnO nanorods [11]. The larger intensity ratio indicates that ZnO nanorods have a less deep level defect concentration. The relative integrated PL intensity ratio ( $I_{UV}/I_{DLE}$ ) of different samples was summarized in the insert image of Fig.3. It can be seen that  $I_{UV}/I_{DLE}$  value shows almost the same value for OZN-A and SZN, which indicates that sealing the beaker during the growth can strongly improve the crystal quality of ZnO nanorods and make it even as good as a 500°C annealed ZnO nanorods grown in an open beaker. Furthermore, it is well known that ZnO grown in the chemical solution has two kinds of defects, i.e. surface defects and intrinsic defects as mentioned above.

The strong enhancement of UV emission of OZN-A and SZN mainly relates to the surface defects due to the slight variation in the DLE band compared with OZN [11].

TRPL is a powerful method to monitor the existence of the surface recombination. As earlier demonstrated for Si epilayer [28-30], the surface recombination can strongly influence the decay time. The excess minority carriers via the near bandgap recombination exhibit a single exponential decay or a non-exponential decay, depending on whether the surface recombination is the major recombination channel or not. Fig.4 shows the low-temperature (1.8K) TRPL spectra from OZN, OZN-A and SZN. The time-resolved signals were recorded with detection wavelength at the maximum intensity of the UV emission peak (around 369.52 nm). All three samples exhibit a non-exponential decay, as shown in Fig.4, which means the surface recombination is the major recombination channel in them. By examining the decay curves in Fig.4, we find that the decay curves can be fitted by two exponential decays:

$$I(t) = A_S e^{-t/\tau_S} + A_B e^{-t/\tau_B} \quad (8)$$

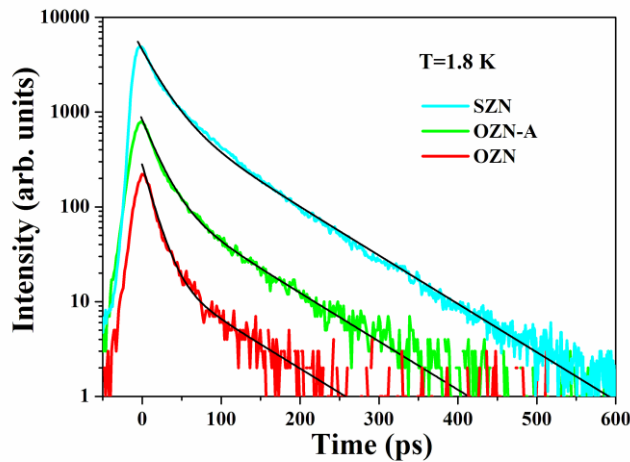


Fig. 4 Decay curves for OZN, OZN-A and SZN. The decays were measured at 1.8 K. The black lines are fitting curve according to Eq. (8).

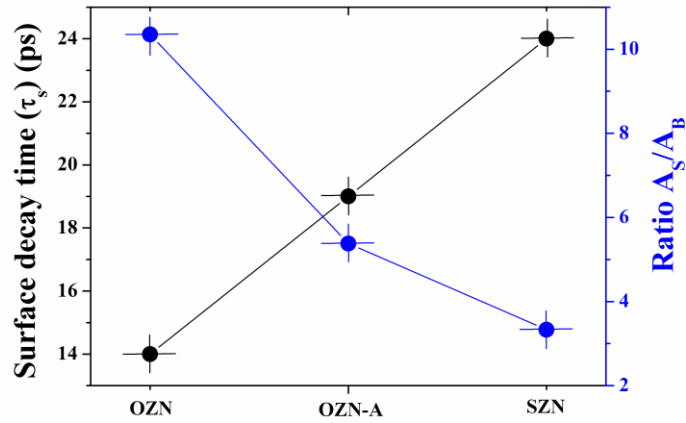


Fig. 5 Deduced values of time constant  $\tau_s$  and ratio  $A_s/A_B$  for OZN, OZN-A and SZN according to Eq. (8).

where  $I(t)$  represents the PL intensity as a function of time, while  $A_S$  and  $A_B$  are the relative weights of the two exponential decays with time constants  $\tau_s$  and  $\tau_B$ , respectively.

The black lines in Fig.4 represent the fitting decay curves according to Eq. (8). The results show that the value of  $\tau_B$  is the same, 95 ps, for all decay curves. We believe that this time constant represents an effective “bulk” exciton decay time in these samples, which has been discussed in detail in our previous reports [10-11]. Apparently, the value of  $\tau_B$  in our case is much shorter compared to other reports on the high-temperature grown ZnO nanorods. For examples, Zhang et al. reported an exciton radiative lifetime of about 340 ps in ZnO nanorods fabricated by a vapor transport method [31]. Recently, Mohanta et al. revealed an exciton radiative lifetime of about 432 ps in ZnO nanorods prepared by metal organic chemical vapor deposition (MOCVD) [32]. For these two techniques, i.e. vapor transport method and MOCVD, the growth temperature is at least 450°C, which is much higher than 93°C in our experiment, so the crystalline quality of their sample is better than our samples, which results in that our exciton radiative lifetime is much shorter. Although our

value is shorter, it is still longer than that (70 ps) from the samples prepared by the other low-temperature (90°C) aqueous chemical growth technique [33], which means our sample has a relatively better crystalline quality. Moreover, the same deduced value of  $\tau_B$  for three samples prepared under different conditions indicates that the crystal qualities of “bulk” parts in them are same. It further reveals that the difference between the three decay curves depends mainly on another fast exponential decay with time constants  $\tau_S$  which is strongly influenced by the surface recombination. The deduced value for time constant  $\tau_S$  and the ratio of  $A_S/A_B$  are summarized in Fig. 5. As seen in Fig. 5,  $\tau_S$  of OZN-A and SZN increases step by step compared with OZN, while the ratio,  $A_S/A_B$ , decreases. These factors indicate that the first term in Eq. (8) becomes less important in influencing the decay time of OZN-A and SZN. This clearly illustrates that sealing the beaker during the growth can effectively suppress the surface recombination of ZnO nanorods and realize an even better impact than a 500°C post-thermal treatment on ZnO nanorods grown in an open beaker.

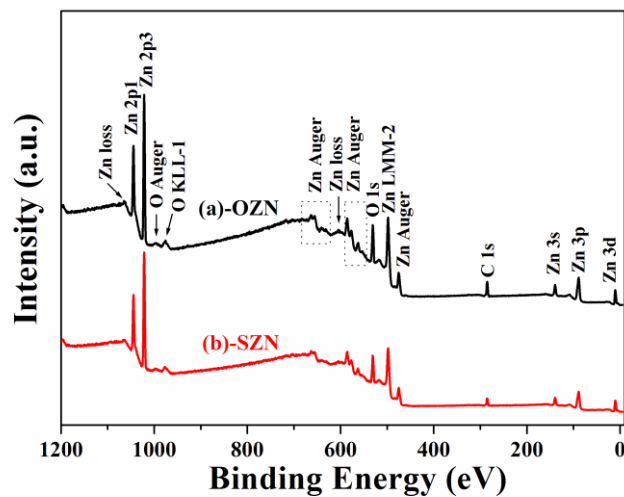


Fig.6 XPS survey spectra of OZN and SZN, where the labels indicated the origin of the corresponding peaks.

To reveal the effect and mechanism of growth process on the surface recombination, it is necessary to understand the surface composition of OZN and SZN. XPS was used to investigate the surface composition of OZN and SZN. Fig. 6 shows the XPS survey spectra obtained from OZN and SZN, in which all of the peaks can only be ascribed to Zn, O, and C elements as labeled in Fig. 6 [34]. It indicates that there are no other impurities observed in both samples. We would like to mention that, in all the XPS spectra of ZNAs, the binding energies have been calibrated by taking the carbon C1s peak (285.0 eV) as reference.

The deconvolutions of the XPS spectra for the O1s core level line from OZN and SZN are shown in Fig. 7(a) and 7(b), respectively. For all XPS spectra in this paper, the open circles denote the experimental data, red solid line represents the fitting curves and the deconvoluted individual peaks are depicted by green lines. In Fig. 7 (a), the deconvolutions show the presence of four different O1s peaks in the OZN. The peak centered at  $530.35 \pm 0.3$  eV (O1) is associated to the  $O^{2-}$  ion in the wurzite structure surrounded by Zn atoms with their full complement of nearest-neighbor  $O^{2-}$  ions [35-44]. The peak at  $531.54 \pm 0.3$  eV (O2) is attributed to the presence of OH bonds, i.e. ZnO(OH) [37-41]. The binding energy peak at  $532.87 \pm 0.3$  eV (O3) can be ascribed to the specifically chemisorbed oxygen, such as  $-CO_3$ , adsorbed  $O_2$ , or adsorbed  $H_2O$  [35-44]. Another peak located at  $528.38 \pm 0.3$  eV (O4) is related to the oxygen from a H-ZnO( $10\bar{1}0$ ) surface as reported in our previous report [45]. In Ref [45], we reported that the OH (O2) and H (O4) bonds play the dominant role in facilitating surface recombination, but specific chemisorbed oxygen (O3) also likely affect the surface recombination. The lower binding energy of O3 located at, the less contribution of the component to the surface recombination. However, in Fig. 7(b), only O1 and O3 components are extracted from the experimental curve and the

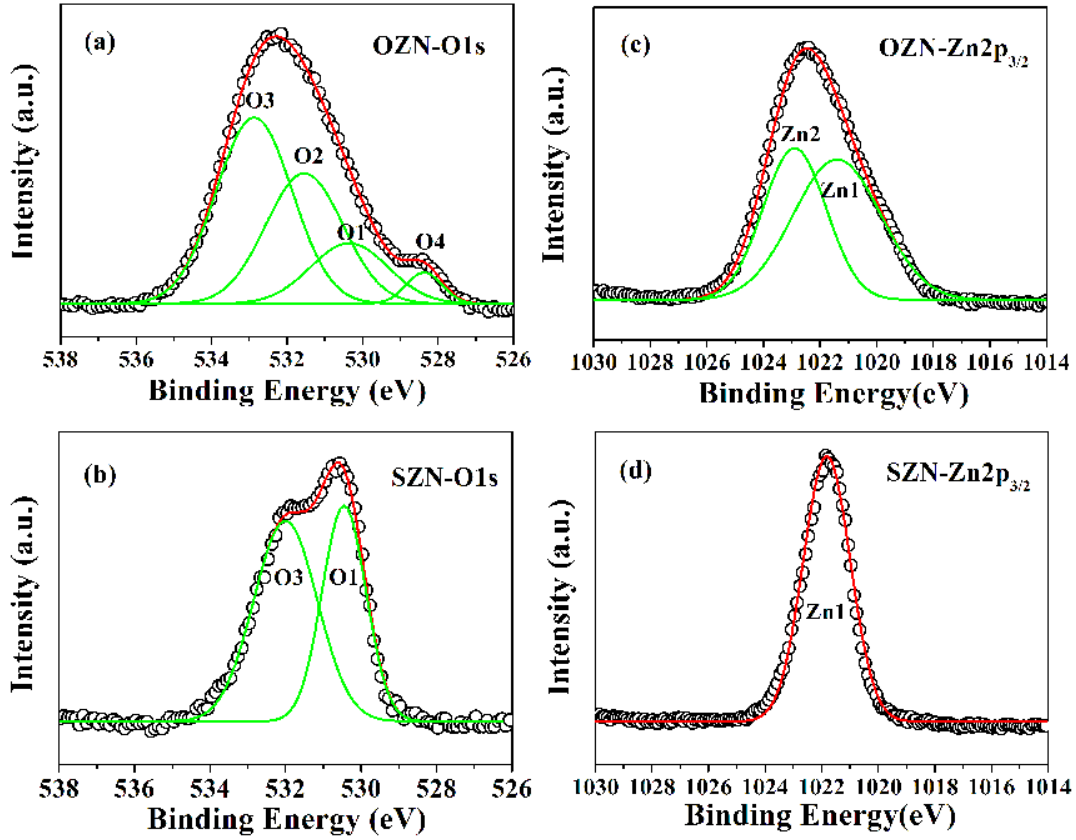


Fig.7 (a) O1s XPS spectrum of OZN where four components (green curves) were used to deconvolute the experimental peak, as labeled by O1, O2, O3 and O4; (b) O1s XPS spectrum of SZN, only O1 and O3 components were extracted from the experimental curve; (c) Zn  $2p_{3/2}$  XPS spectrum of OZN, where two components (green curves) were used to deconvolute the experimental peak, as labeled by Zn1 and Zn2; (d) Zn  $2p_{3/2}$  XPS spectrum of SZN, only Zn1 component was extracted from the experiment curve.

binding energy of O3 ( $532.12 \pm 0.3$  eV) in SZN is lower by about 0.75 eV than that in OZN, which has less contribution to the surface recombination process. Therefore, the O1s XPS results indicate that surface defects, such as O2, O3 and O4 which do great contribution to the surface recombination, are strongly suppressed by sealing the beaker during the growth process. Furthermore, the deconvolutions of the XPS spectra for the Zn  $2p_{3/2}$  core level line from OZN and SZN are shown in Fig. 7(c) and 7(d), respectively. The Zn  $2p_{3/2}$  XPS spectrum from OZN is very broad and asymmetric. A good fit to the experimental data only could be obtained when deconvolutions of two Gaussians were used for the spectrum, which indicates that two

zinc species exist on the surface of OZN. The observed peak with binding energy of  $1021.42 \pm 0.3$  (Zn1) is associated to Zn species in ZnO [46-47]. The other peak with binding energy of  $1022.91 \pm 0.3$  (Zn2) corresponds to Zn species ( $1022.73$ ) in ZnO(OH) according to Ref.[48-50]. However, for SZN, only Zn1 is enough to fit the experiment curve. This indicates that ZnO(OH) either does not exist on the surface of SZN or the concentration is too low to be detected by XPS, which further testifies the O1s XPS results. Therefore, the XPS results indicate that OH and H groups dominate the surface of OZN, while a totally different situation happens on the surface of SZN. This phenomenon depends on the different growth mechanism of OZN and SZN, which will be discussed in detail in the following part.

According to the reaction formulae (1)-(7) of OZN, four coordinated Zn cation largely occurs as tetrahedral complexes [51]. Therefore, two complexes,  $\text{Zn}(\text{NH}_3)_4^{2+}$  and  $\text{Zn}(\text{OH})_4^{2-}$ , are generated in the solution and become the precursors of ZnO. Some  $\text{Zn}(\text{NH}_3)_4^{2+}$  and  $\text{Zn}(\text{OH})_4^{2-}$  will exist on the outside surface of OZN since the sample are interruptedly taken out from the chemical solution and form the surface defects to provide the surface recombination centers. On the contrary, for SZN, when the beaker is sealed, the obvious and pivotal difference compared with an open beaker is the concentration of  $\text{NH}_3$  in the solution. With opening the beaker, most part of the  $\text{NH}_3$  will evaporate from the solution so that  $\text{Zn}(\text{OH})_4^{2-}$  is the main precursors of ZnO. But with sealing the beaker, all the  $\text{NH}_3$  will be kept in the beaker. Thus, two factors should be taken account for the reaction. On one hand, more  $\text{NH}_3$  will participate in the reaction according to chemical formula (4), so more  $\text{Zn}(\text{NH}_3)_4^{2+}$  precursors forms on the surface of ZnO nanorods. On the other hand, more groups related to  $\text{NH}_3$  are absorbed by the surface of ZnO nanorods due to the high concentration of  $\text{NH}_3$  in the beaker. Therefore, we deduce that the group related to  $\text{NH}_3$  is the main group attached

on the surface of SZN, which may have less contribution on the surface recombination. In order to verify this, XPS was used to detect the nitrogen signal from the OZN and SZN. Fig.8 shows the N1s XPS spectra from OZN and SZN. From Fig.8, we can see that one peak located at  $400.02 \pm 0.3$  eV can be observed in both samples. It is known that the N 1s peak from molecularly adsorbed  $\text{NH}_3$  on metal and semiconductor surfaces appears at 400-401 eV, whereas for the partially decomposed species, i.e.,  $\text{NH}_x$  ( $x=1, 2$ ), N 1s peak appears at 398-399.4 eV [52-54]. Thus, the peak at 400.02 eV is well associated with the molecularly adsorbed  $\text{NH}_3$ , which proves that the groups associated to  $\text{NH}_3$  indeed cover the surface of SZN as induced above. But we can also observe that the relative intensity of N1s signal from SZN is about three times of that from OZN. This implies that more groups related to  $\text{NH}_3$  are attached on the surface of SZN.

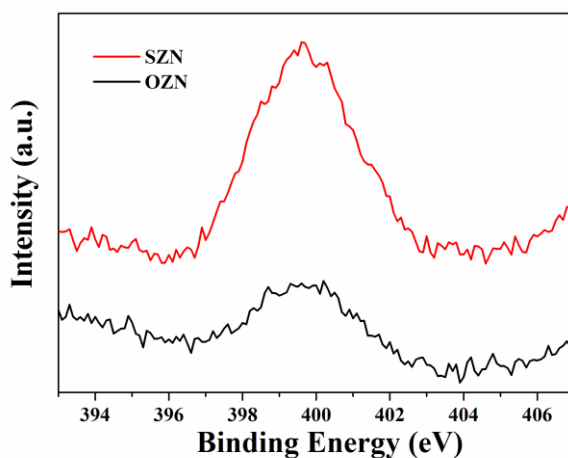


Fig.8 N1s XPS spectra of OZN and SZN.

To further reveal the effect of  $\text{NH}_3$  absorbed by the surface on the optical properties of ZnO nanorods, ammonia was used to perform surface modification on the as-grown OZN and SZN. For protecting the surface morphology to make it the same as the as-grown nanorods, low concentration of ammonia solution (0.1M) and

short time (15min) treatment were used in the experiments. In addition, the experiment was carried out at 93°C as the growth condition, which aimed to simulate the growth condition for the easier comparison and analysis. The room-temperature PL spectra from OZN, OZN-N, SZN and SZN-N are shown in Fig.9. As shown in Fig.9 (a), after ammonia treatment, the UV emission intensity of OZN-N is enhanced compared with OZN. While the intensity of the DLE band shows almost no change, indicating that the surface treatment does not influence the concentration of deep level defects. Thus, the enhancement of the UV emission is mainly related to the surface treatment by ammonia. When the OZN is immersed in the ammonia solution, two actions will happen in the solution. On one hand,  $Zn(OH)_4^{2-}$  on the surface will follow the reaction formula (7) to decompose into ZnO, which will enhance the intensity of the UV emission as shown for the OZN-N sample. On the other hand, due to the short time treatment under low concentration of ammonia solution, the surface morphology of OZN-N is same as OZN, which indicates that a devastating etching process does not happen on the surface. But 15min is enough for the whole surface to

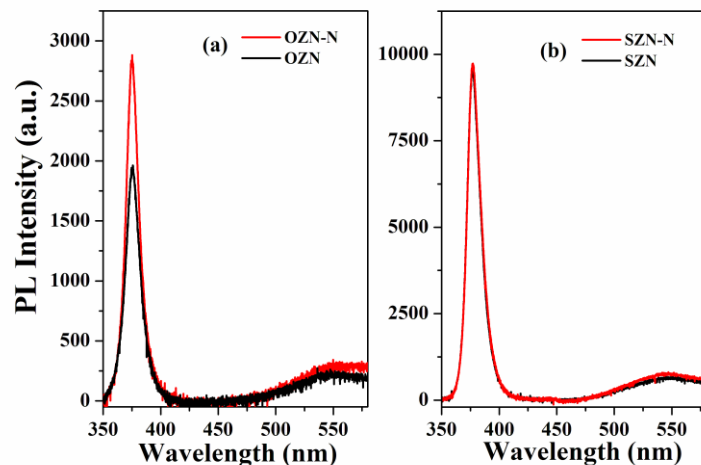


Fig.9 (a) Room-temperature PL spectra from OZN and OZN-N; (b) Room-temperature PL spectra from SZN and SZN-N.

be attached by the groups related to  $\text{NH}_3$ . From this aspect, we can know that the absorption of the groups related to  $\text{NH}_3$  not only does not introduce the surface recombination into the emission process, but also even benefit for the enhancement of the emission intensity of ZnO nanorods. Furthermore, we performed the same treatment on the SZN. As shown in Fig.9 (b), after ammonia treatment, the PL spectra from SZN and SZN-N are almost the same. It indicates that the quantity of  $\text{NH}_3$  on the SZN surface is already saturated during the growth process so that no more  $\text{NH}_3$  can be attached in the ammonia treatment. Hence, the optical property of SZN is better than OZN. Martins et al had calculated the highest occupied molecular orbital (HOMO) energy, lowest unoccupied molecular orbital (LUMO) energy and HOMO-LUMO band gap of  $\text{NH}_3$  molecule absorbed by  $(\text{ZnO})_{22}$  cluster [55]. The band gap diagram is illustrated in Fig.10. It can be seen that the LUMO and HOMO energy level of  $\text{NH}_3$  are both beyond the band gap, indicating that  $\text{NH}_3$  attachment can not form surface state in the ZnO nanorods. Besides, the small energy barriers formed at valence band and conduction band make the electron and hole effectively combined and enhance the emission efficiency. So far, the theoretical calculation and

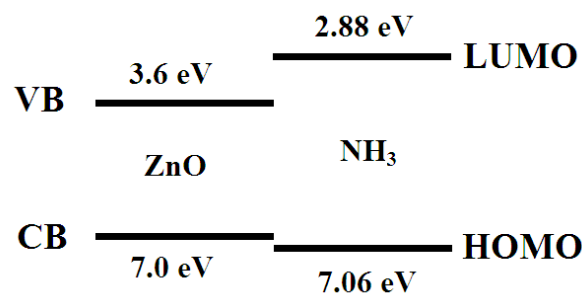


Fig. 10 Band gap diagram of ZnO attached by  $\text{NH}_3$ . All the energy values are the relative value to the vacuum level. The position of LUMO and HOMO were taken from the calculation [55]. The position of VB and CB of ZnO were taken from the experiment [56].

experimental measurement about the LUMO and HOMO energy level of  $\text{NH}_3$  absorbed by ZnO are still limited. We hope that our results can stimulate more investigations on it.

## **Conclusion**

In the paper, we present an effective way, i.e. sealing the beaker, to suppress the surface recombination during the growth process, which can realize a better impact than a  $500^\circ\text{C}$  post-thermal treatment on ZnO nanorods grown in the open beaker. The results also reveal that the absorption of the groups related to  $\text{NH}_3$  by the surface of ZnO nanorods has no contribution to the surface recombination during the optical emission process. This work not only simplifies the preparation procedure of ZnO nanorods arrays with high crystal quality and save the cost for large-scale fabrication, but also provides an easier way to improve the properties of photoelectronic devices.

## **Acknowledgements**

The authors would like to acknowledge financial support for this work from the Swedish Research Council (VR) and financial support through Swedish Research Links via VR. L.L. Yang would also like to acknowledge financial support from National Nature Science Foundation of China (NNSFC, No.60878039 and 60778040), program for the development of Science and Technology of Jilin province (Item No. 20090140) and the Eleventh Five-Year Program for Science and Technology of Education Department of Jilin Province (Item No. 20080156).

## References

- (1) Huang M. H.; Mao S. ; Feick H. ; Yan H.; Wu Y. ; Kind H. ; Weber E. ; Russo R. ; Yang P. *Science* **2001**, 292, 1897.
- (2) Johnson J. C.; Choi H. J.; Knutsen K. P.; Schaller R, D.; Yang P.; Saykally R. J. *Nat. Mater.* **2002**, 1, 106.
- (3) Duan X.; Huang Y.; Agarwal R.; Lieber C. M. *Nature (London)* **2003**, 421, 241.
- (4) Law M.; Sirbully D. J.; Johnson J. C.; Goldberger J.; Saykally R. J.; Yang P. *Science* **2004**, 305, 1269.
- (5) Barrelet C. J.; Greytak A. B.; Lieber C. M. *Nano Lett.* **2004**, 4, 1981.
- (6) Greytak A. B.; Barrelet C. J.; Li Y.; Lieber C. M. *Appl. Phys. Lett.* **2005**, 87, 151103.
- (7) Willander M.; Yang L L.; Wadeasa A.; Ali S. U.; Asif M. H.; Zhao Q. X.; Nur O. *J. Mater. Chem.* **2009**, 19, 1006.
- (8) Pan N.; Wang X. P.; Ming L.; Li F.Q.; Hou J.G. *J. Phys. Chem. C* **2007**, 111, 17265.
- (9) Shalish I.; Temkin H.; Narayanamurti V. *Physical Review B* **2004**, 69, 245401.
- (10) Zhao Q. X.; Yang L. L.; Willander M.; Sernelius B. E.; Holtz P. O. *J. Appl. Phys.* **2008**, 104, 073526.
- (11) Yang L. L.; Zhao Q. X.; Willander M.; Yang J. H. and Ivanov I. *J. Appl. Phys.* **2009**, 105, 053503.
- (12) Yang L. L.; Zhao Q. X.; Willander M. *J. Alloys and Compounds* **2009**, 469, 623.
- (13) Yang L. L.; Zhao Q. X.; Willander M.; Yang J. H. *J. Crystal Growth* **2009**, 311 1046.
- (14) Li Q. C.; Kumar V.; Li Y.; Zhang H. T.; Mark T. J.; Chang R. P. H.; *Chem. Mater.* **2005**, 17,1001-1006

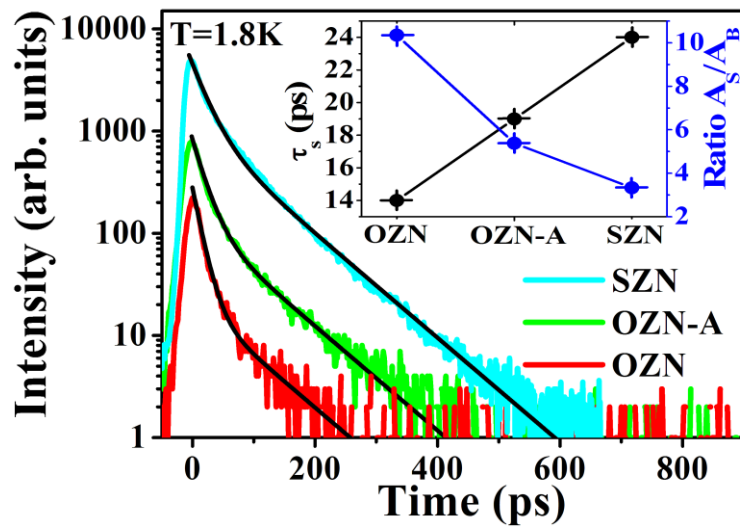
- (15) Gao X. D.; Li X. M.; Yu W. D.; *J. Phys. Chem. B* **2005**, *109*, 1155-1161
- (16) Yu L.; Zhang G. M.; Li S. Q.; Xi Z. H.; Guo D. Z.; *J. Cryst. Growth* **2007**, *299*, 184-188
- (17) Kasai P. H. *Phys. Rev.* **1963**, *130*, 989.
- (18) Vanheusden K.; Warren W. L.; Seager C. H.; Tallant D. R.; Voigt J. A.; and Gnade B. E. *J. Appl. Phys.* **1996**, *79*, 7983.
- (19) Yamauchi S.; Goto Y.; Hariu T. *J. Cryst. Growth* **2004**, *260*, 1.
- (20) Liu M.; Kitai A. H.; Mascher P. *J. Lumin.* **1992**, *54*, 35.
- (21) Bylander E. G. *J. Appl. Phys.* **1978**, *49*, 1188.
- (22) Yang X.; Du G.; Wang X.; Wang J.; Liu B.; Zhang Y.; Liu D.; Liu D.; Ong H. C.; Yang S.; *J. Cryst. Growth* **2003**, *252*, 275.
- (23) Zhong J.; Kitai A. H.; Mascher P.; Puff W. *J. Electrochem. Soc.* **1993**, *140*, 3644.
- (24) Johnston K.; Henry M. O.; Cabe D. M.; Agne T.; Wichert T. *Proceedings of the Second Workshop on "SOXESS European Network on ZnO, 27-30 October 2004, Caernarfon, Wales, UK.*
- (25) Zhao Q. X.; Klason P.; Willander M. *Appl. Phys. Lett.* **2005**, *87*, 211912.
- (26) Børseth T. M.; Svensson B. G.; Kuznetsov A. Yu.; Klason P.; Zhao Q. X.; Willander M. *Appl. Phys. Lett.* **2006**, *89*, 262112.
- (27) Klason P.; Børseth T. M.; Zhao Q. X. *Solid State Communication* **2008**, *145*, 321.
- (28) Luke K. L.; Cheng L. J. *J. Appl. Phys.* **1987**, *61*, 2282.
- (29) Buczkowski A.; Radzinski Z.J.; Rozgonyi G.A.; Shimura F. *J. Appl. Phys.* **1991**, *69*, 6495.

- (30) Thölmann K.; Yamaguchi M.; Yahata A.; Ohashi H. *Jpn. J. Appl. Phys.* **1993**, 32, 1.
- (31) Zhang X. H.; Chua S. J.; Yong A. M.; Yang H. Y.; Lau S. P.; Yu S. F.; Sun X.W.; Miao L.; Tanemura M.; Tanemura S. *Appl. Phys. Lett.* **2007**, 90, 013107.
- (32) Mohanta S. K.; Tripathy S.; Zhang X. H.; Kim D. C.; Soh C. B.; Yong A. M.; Liu W.; Choi H. K. *Appl. Phys. Lett.* **2009**, 94, 041901.
- (33) Bekeny C.; Voss T.; Hilker B.; Gutowski J.; Hauschild R.; Kalt H.; Postels B.; Bakin A.; Waag A. *J. Appl. Phys.* **2007**, 102, 044908.
- (34) Yong B. S.; Chul C. H.; Woong N. C.; Jeunghee P. *Appl. Phys. Lett.* **2005**, 86, 033102.
- (35) Meng L. J.; Moreira C. P.; Santos M, P, *Appl. Surf. Sci.* **1994**, 78, 57.
- (36) Lu Y. F.; Ni H. Q.; Mai Z. H.; Ren Z. M. *J. Appl. Phys.* **2000**, 88, 498.
- (37) Rosa E De la.; Seplveda-Guzman S.; Reeja-Jayan B.; Torres A.; Salas P.; Elizondo N.; Yacaman M. *J. J. Phys. Chem. C* **2007**, 111, 8489.
- (38) Wang H. H.; Baek S. H.; Song J. J.; Lee J. H.; Lim S. W. *Nanotechnology* **2008**, 19, 075607.
- (39) Meng L. J.; Moreira de Sa C. P.; Dos Santos M. P. *Appl. Surf. Sci.* **1994**, 78, 57.
- (40) Boulares N.; Guergouri K.; Zouaghi R.; Tabet N.; Lusson A.; Sibieude F.; Monty C. *Phys. Status Solidi A* **2004**, 201–210, 2319.
- (41) Toumiat A.; Achour S.; Harabi A.; Tabet N.; Boumaour M.; Maallemi M. *Nanotechnology* **2006**, 17, 658.
- (42) Chen M.; Wang X.; Yu Y. H.; Pei Z. L.; Bai X. D.; Sun C.; Huang R. F.; Wen L. *S. Appl. Surf. Sci.* **2000**, 158, 134.
- (43) Coppa B. J.; Davis R. F.; Nemanich R. J. *Appl. Phys. Lett.* **2003**, 82, 400.
- (44) Wang H. H.; Xie C. S. *Physica E* **2008**, 40, 2724.

- (45) Yang L. L.; Zhao Q. X.; Willander M.; Liu. X. J.; Fahlman M.; Yang J. H. *Appl. Surf. Sci.* doi:10.1016/j.apsusc.2009.12.160.
- (46) Ramgir N. S.; Late D. J.; Bhise A. B.; More M. A.; Mulla I. S.; Joag D. S.; Vijayamohanan K. *J. Phys. Chem. B* **2006**, *110*, 18236.
- (47) Leunga C. Y.; Djurišić A. B.; Leung Y. H.; Ding L.; Yang C. L.; Ge W. K. *J. Crystal Growth* **2006**, *290*, 131.
- (48) Crist B. V. *Handbooks of Monochromatic XPS spectra - Vol.2 - Commercially Pure Binary Oxides*, XPS International Inc., 1999, pp820.
- (49) Umabayashi R.; Akao N.; Hara N.; Sugimoto K. *J. Electrochemical Society* **2003**, *150*, B295.
- (50) Pettenkofer C.; Meier U. *Appl. Surf. Sci.* **2005**, *252*, 1139.
- (51) Lee J.D.; *Concise Inorganic Chemistry*; fourth ed.; Chapman & Hall: London, 1991; pp 845.
- (52) Moulder J. F.; Stickle W. F.; Sobol P. E.; Bomben K. D. *Handbook of X-ray Photoelectron Spectroscopy*; Perkin-Elmer Corporation: Eden Prairie, 1992.
- (53) Perkins C. L.; S. H. Lee.; Li X.N.; Asher S. E.; Coutts T. J. *J. Appl. Phys.* **2005**, *97*, 034907.
- (54) Ozawa K.; Hasegawa T.; Edamoto K.; Takahashi K.; Kamada M. *J. Phys. Chem. B* **2002**, *106*, 9380.
- (55) Martins J.B.L.; Longo E.; Taft C.A. *J. Quan. Chem.* **1998**, *70*, 367.
- (56) Wadeasa A.; Nur O.; Willander M. *Nanotechnology* **2009**, *20*, 065710.

## Effective suppression of surface recombination in ZnO nanorods arrays during the growth process

*L.L. Yang*<sup>\*,†,‡</sup>, *Q.X. Zhao*<sup>†</sup>, *M. Willander*<sup>†</sup>, *X.J. Liu*<sup>§</sup>, *M. Fahlman*<sup>§</sup>, *J.H. Yang*<sup>‡</sup>



Low temperature (1.8K) decay curves for OZN, OZN-A and SZN are fitted by two exponential decays according to the equation  $I(t) = A_S e^{-t/\tau_S} + A_B e^{-t/\tau_B}$ . The insert indicate that sealing the beaker during the growth process can effectively suppress the surface recombination of ZnO nanorods and the suppression effect is even better than a 500°C post-thermal treatment to OZN.